Preferential Light Absorption in Atheromas In Vitro

Implications for Laser Angioplasty

Martin R. Prince, Thomas F. Deutsch, Micheline M. Mathews-Roth,* Randy Margolis, John A. Parrish, and Allan R. Oseroff
Wellman Laboratory of Photomedicine, Massachusetts General Hospital, Harvard Medical School, Boston, Massachusetts 02114; and
**Channing Laboratory, Brigham and Women's Hospital, Harvard Medical School, Boston, Massachusetts 02115*

Abstract

Laser angioplasty, the in situ ablation of arterial obstructions with laser radiation, has been demonstrated in animal models and early clinical trials. A problem with this technique, however, is the possibility of thermal damage to adjacent or underlying normal tissues that also absorb the radiation. Using a spectrophotometer with an integrating sphere and a specially constructed tunable-dye laser-based spectrophotometer, we evaluated the transmittance and remittance of human cadaveric atheromas and adjacent normal aorta from 250 to 1,300 nm to identify wavebands where there is preferential light absorption by atheromas. Data were analyzed by both the Kubelka-Munk formalism and a Beer's law model. Both methods indicate that atheromas absorb more than normal aorta between 420 and 530 nm. At 470 nm the average Kubelka-Munk absorption coefficient of atheromas from 10 cadavers was 54±9 cm^{-1} compared with 26±6 cm^{-1} for normal aortic specimens from seven cadavers. Yellow chromophores responsible for the atheroma absorbance were extractable with xylenes. Thin-layer chromatography and absorption spectra identified the extracted chromophores as predominantly consisting of a mix of carotenoids, which are known constituents of atheromatous lesions. Preferential absorption of blue light by carotenoids in atheromas may permit selective ablation of atheromatous obstructions with appropriate pulses of laser radiation.

Introduction

Laser angioplasty, the ablation of arterial obstructions with laser light, has been demonstrated in vitro (1–9), in animals (10–18), and in early clinical trials (19–23). While these studies have shown the feasibility of this technique, clinical application has been limited by vessel perforations, aneurysms, and other forms of inadvertant laser damage to normal tissue adjacent to or underlying the atheromas (11, 12, 14–17, 22, 23). Laser angioplasty would be enhanced if the light energy could be selectively deposited in the obstructing material rather than in normal tissue. This could be accomplished by choosing a waveband in which the atheroma has a higher absorbance than that of the adjacent normal tissue.

It is evident from inspection of atheromas that they differ in color from normal artery. We chose to evaluate the optical properties of atheromas and normal vascular tissues to identify wavebands of preferential absorption in atheromas and the responsible chromophores. Little previous work has been done in this area. Kaminow et al. measured direct transmittance of plaque specimens in a spectrophotometer and reported increased absorption at the shorter visible and ultraviolet wavelengths (24). However, there was no attempt to compare atheroma transmittance with that of normal vascular tissues. In addition, with the exception of hemoglobin absorbances, the data showed no defined absorption bands associated with the atheromas. Van Gemert et al. measured remittance and transmittance using an integrating sphere detection system and three common lasers (argon, helium-neon, and yttrium aluminum garnet) as light sources (25). Absorption and scattering coefficients were calculated using the Kubelka-Munk model (26–29). Although they noted some preferential absorption in atheromas at argon (514 nm) and Nd:yttrium aluminum garnet (1,060 nm) laser lines, having only three data points prevented the identification of wavebands of maximum preferential absorption.

In this study two techniques were used to evaluate tissue absorption. First, remittance and transmittance were measured on a spectrophotometer fitted with an integrating sphere, and the Kubelka-Munk (KM)[1] model for light propagation in scattering media was used to calculate absorption coefficients (26–29). The integrating sphere measurements had reduced precision in regions of high absorbance, which were the regions of greatest interest. Accordingly, a tunable-dye laser-based spectrophotometer was constructed that could accurately measure transmittance to 10^{-3}% through tissue samples irradiated over areas as small as 1 mm^2 (30). After identifying the spectral regions of preferential absorption in atheromas, we extracted and partially characterized the responsible chromophores.

Methods

Specimens. Portions of human aorta were obtained from 10 cadavers less than 48 h postmortem. Optical measurements with the integrating sphere were made on six soft, yellow, raised plaques from which the outer portion of the media and adventitia had been stripped by blunt dissection. Each plaque came from a different cadaver and was measured once. A total of seven normal aorta specimens were prepared from three of the cadavers. One was studied as an intact full-thickness specimen and measured three times. A second was studied intact and then roughly divided into adventitia, media, and intima by blunt dissection, and the integral parts were examined separately. A third was divided into an intimal and a medial specimen before measurement. Laser spectrophotometer measurements were made on specimens from four cadavers. In

This work was presented in part at the national meeting of the American Federation of Clinical Research, Washington, DC, 3 May 1985; and was published in abstract form, 1985. *Clin. Res.* 33:218A.

Address reprint requests to Dr. Prince, Wellman 2, Massachusetts General Hospital, Fruit St., Boston, MA 02114.

Received for publication 16 July 1985 and in revised form 13 March 1986.

J. Clin. Invest.

0021-9738/86/07/0295/08 $1.00
Volume 78, July 1986, 295–302

1. *Abbreviations used in this paper:* A_B, Beer's law absorption coefficient; *D*, thickness; *I*, into; *J*, outwards; *K*, absorption coefficient; KM, Kulbeka-Munk; *R*, remittance; *S*, scattering coefficient; *T*, transmittance.

each specimen, three atheromatous regions and three adjacent normal spots were studied, for a total of 12 pairs of measurements.

Integrating sphere measurements. Specimens of 0.2–2 mm in thickness were mounted in a holder with polished quartz windows that was filled with normal saline to minimize optical artifacts from tissue surface irregularities. The air-quartz interfaces of the holder had a consistent and predictable on-axis remittance that was measured and subtracted from the tissue remittance measurement. The mounted tissue was placed on a 7.5-cm diameter barium sulfate–coated integrating sphere connected by 2-mm i.d. fiber optic bundles to a 5270 double-beam spectrophotometer (Beckman Instruments, Inc., Fullerton, CA) as shown in Fig. 1 and as described previously (31–33). This spectrophotometer was interfaced to a 9825A computer (Hewlett-Packard Co., Palo Alto, CA) for digital data acquisition and analysis. The apparatus used a collimated light beam to illuminate a 5-mm diameter region of the sample tissue. Diffuse illumination was not used because it would have required illumination of a spot substantially larger in diameter, making it difficult to study individual discrete atheromas. The illumination wavelength was scanned from 1,330 to 250 nm. Freshly coated barium sulfate plates were used as 100% remittance standards. Thickness of the tissue positioned between the two quartz windows was measured with a micrometer. To examine the effect of denaturation on tissue optics, some mounted specimens were heated with a hot air gun to 100°C and remeasured.

Immediately after measurement of remittance and transmittance, the area examined was marked with india ink, fixed in 10% buffered formalin, processed through xylene and graded alcohols, and paraffin embedded. Sections were stained with hemotoxylin and eosin for light microscopy. Silver stains were used on selected sections to better visualize elastic fibers.

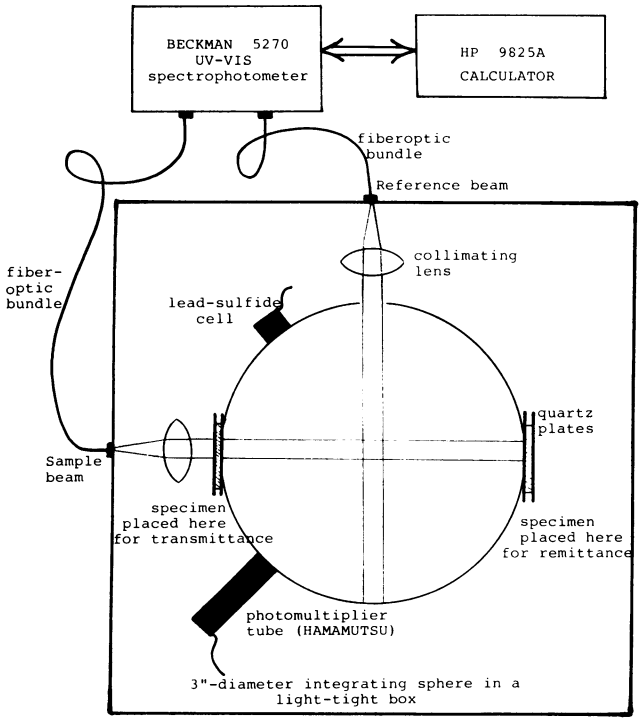

Figure 1. Integrating sphere/spectrophotometer apparatus. Light from a conventional spectrophotometer is conducted to the integrating sphere via fiberoptic bundles and detected using either a lead sulfide cell (infrared) or a photomultiplier tube (UV and visible). Tissue transmittance is measured by placing tissue in the path of the sample beam where light enters the integrating sphere on the left, and by covering the exit hole with a plate coated with barium sulfate. Remittance is measured by placing the specimen in the path of the sample beam where light exits the integrating sphere on the right.

Laser-based spectrophotometer measurements. Because the integrating sphere measurements were limited to transmittance > 0.5% and to a 5-mm diameter region on the samples, a tunable-dye laser-based spectrophotometer was constructed that could measure transmittances as low as 10^{-3}% in 1-mm diameter spots (30). This device is shown schematically in Fig. 2. The small spot size permitted direct comparison of optical properties at adjacent normal and atheromatous regions on the same specimen. The specimens were immersed in normal saline during measurements to minimize the effects of irregular surface contours and to simulate the in vivo optical environment.

A nitrogen-laser–pumped dye laser (Laser Sciences, Inc., Cambridge, MA) was used to provide light from 400 to 605 nm using diphenylstilbene, coumarin 440, coumarin 480, coumarin 540A, and rhodamine 6G dyes. Direct and indirect transmitted light was detected with a 1 cm^2 UV-IR enhanced silicon photodiode (No. 1337-1010BQ; Hamamatsu, Corp., Middlesex, NJ). A resistance-capacitance integrating circuit was used to average over 100 laser pulses. A reference beam with an identical detection circuit was used to compensate for pulse to pulse variations in laser output. Another identical detection circuit was submerged in the saline bath over the specimen to measure remittance. Remittance measurements were calibrated using a 1.5-mm thick piece of teflon. After measurements the spots studied were marked and processed as above.

Kubelka-Munk analysis. Absorption and scattering coefficients were calculated with the KM model for light propagation in turbid and absorbing media (26–29). In this model, light in the tissue is separated into two diffuse fluxes propagating into (I) and outwards (J) in the sample (Fig. 3). The model defines absorption (K) and back scattering (S) coefficients and describes light propagation by two first order differential equations (Eq. 1 and 2).

$$\frac{dI}{dX} = -SI - KI + SJ \quad (1)$$

$$\frac{dJ}{dX} = SJ + KJ - SI \quad (2)$$

These equations have been solved for the boundary conditions illustrated in Fig. 3 to give the K and S coefficients in terms of the measurable quantities of remittance (R), transmittance (T), and thickness (D) (27).

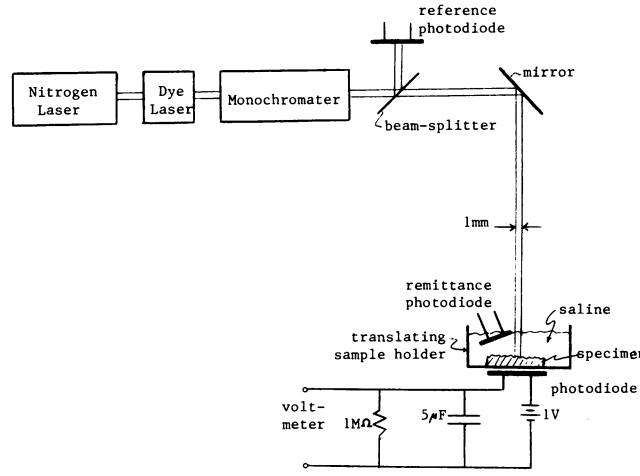

Figure 2. Laser-based spectrophotometer. This spectrophotometer permits multiple measurements on areas as small as 1-mm diameter with transmittance ≥ 10^{-3}%. The tissue is immersed in normal saline to approximate the in vivo optical environment.

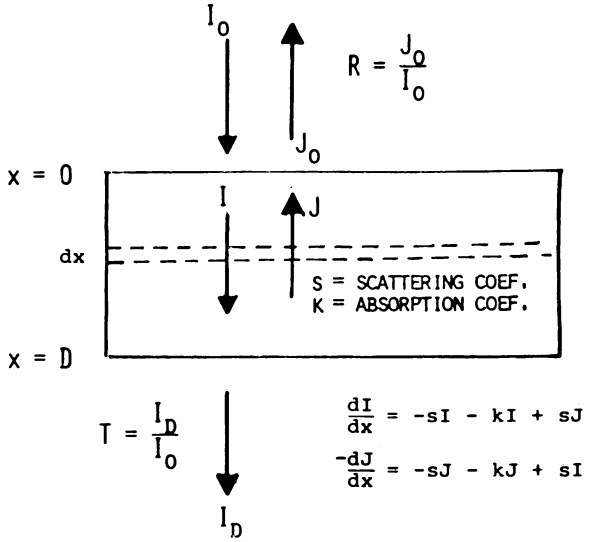

Figure 3. The KM model. Light is assumed to be propagating diffusely through tissue where I_0 is the incident light, J_0 is the remitted light, I_D is the transmitted light, and D is the specimen thickness. By considering a differential element, dx, it is possible to describe the change in I and J with the differential equations shown. These equations can then be solved for the given boundary conditions to give absorption and scattering coefficients in terms of the measurable quantities, remittance, transmittance, and thickness. Boundary conditions: I_0, = incident radiation; I_D/I_0, transmittance; J_D, 0; J_0/I_0, remittance.

$$S = \frac{1}{D}\left[\left(\frac{1 + R^2 - T^2}{2R}\right)^2 - 1\right]^{-1/2} \times \coth^{-1}\left[\frac{\frac{1 - R^2 + T^2}{2R}}{\left[\left(\frac{1 + R^2 - T^2}{2R}\right)^2 - 1\right]^{1/2}}\right] \quad (3)$$

$$K = S\{[(1 + R^2 - T^2)/2R] - 1\} \quad (4)$$

When T is small, Eq. 4 can be approximated by Eq. 5.

$$K = S[(1 - R)^2/2R] \quad (5)$$

For a very small T, such as in a thick specimen or in a region of high absorption, the value of S in Eq. 3 is very sensitive to errors in the measurement of T. Because scattering is usually slow to vary with wavelength (33, 34), it is possible to calculate K using the measured R, and the S from an adjacent spectral region with a higher T. In regions of $T < 0.5\%$, K was calculated in this manner.

Beer's law analysis. In the waveband of preferential absorption in atheromas an additional method was used to evaluate absorption. Beer's law absorption coefficients (A_B) were calculated using Eq. 6.

$$A_B = -\ln(T)/D \quad (6)$$

The ratio of atheroma A_B to normal aorta A_B was plotted to locate the wavelength of maximum preferential absorption in atheromas. This simple analysis ignores the effect of light scattering within the tissue and thus is most accurate in wavebands where scattering is small compared with absorption.

Statistical analysis. Because of the absorption spectra of the yellow atheroma extract, we chose 470 nm as the optimal wavelength for evaluating the statistical significance of observed differences in absorption between atheromatous and normal aorta. The laser spectrophotometer data were treated as paired, since both atheroma and normal aorta were studied for each individual. Because the individual to individual variability was greater than the site to site variability within individuals, the three measurements on the atheromatous and on the normal regions of each of the specimens were averaged, and the average atheroma and normal absorption coefficients for each individual were treated as one pair of observations. Student's t test was used to calculate a P value for the null hypothesis. The t test was also used to calculate a P value for the integrating sphere data alone and pooled with the laser spectrophotometer data. For these calculations the data within individuals was still averaged but was treated as unpaired because of the unequal sample sizes.

Chromophore identification. Lipophilic pigments were extracted by shaking 1.2 g of atheroma or normal aorta in 10 ml common xylenes (X-5 SK; Fisher Scientific Co., Pittsburgh, PA) for 12 h at 5°C. After filtration (No. 42 ashless filter paper; Whatman Inc., Clifton, NJ), absorption spectra of the filtrate were determined in 1-cm path cuvettes using a 5270 UV-VIS spectrophotometer (Beckman Instruments, Inc.). The xylene extracts were then evaporated to 0.2 ml, chromatographed on silica gel thin-layer sheets (Eastman Kodak Co., Rochester, NY) and developed with petroleum ether (boiling point, 30–60°C; No. E139; Fisher Scientific Co.). The spots were cut out and eluted with ethanol. The absorption spectra were measured from 300 to 600 nm on a Cary model 14 spectrophotometer (Varian Associates, Inc., Palo Alto, CA).

Results

Fig. 4 *A* shows the integrating sphere measurement of spectral remittance and transmittance for a typical specimen of intima (310-μm thick) from normal aorta. The calculated KM absorption and scattering coefficients of this specimen are given in Fig. 4 *B*. Comparable data for a typical atheroma (1.5-mm thick) are shown in Fig. 4 *C* and *D*. The greater thickness of this sample gives lower transmittance and higher remittance compared with the sample of normal aorta. On the specimen measured three times there was only a small percentage of variation in measured remittance and transmittance and even less in the calculated absorption and scattering coefficients. The subdivided full-thickness specimen of normal aorta showed no differences in the shape of the absorption and scattering spectra among the three parts: intima, media, and adventicia (data not shown).

Fig. 5 *A* shows the average KM absorption coefficient for integrating sphere measurements on six atheromas compared with that of the seven normal specimens. These spectra exhibit the presence of known tissue chromophores, including hemoglobin (alpha band at 550–570 nm, beta band at 530–550 nm, Soret band at 390–420), aromatic amino acids, and DNA (250–290 nm). The atheroma and normal data do not differ significantly for most of the spectral range covered by the two curves. However, in the region of 420 to 530 nm, the atheromas clearly absorb more than the normal tissues. At 470 nm, the average KM absorption of the six atheromas was 50±7 cm^{-1}, while that of the normal specimens was 24±7 cm^{-1} (Table I). Using a Beer's law analysis which accounts for only the transmitted radiation, the average absorption was 63±7 cm^{-1} for atheroma, compared with 36±7 cm^{-1} for normal.

The laser spectrophotometer data taken in the range of 400–605 nm were similar to the integrating sphere results for all 24 samples from the four cadavers. Fig. 5 *B* shows the calculated KM absorption coefficients for three 1-mm diameter normal

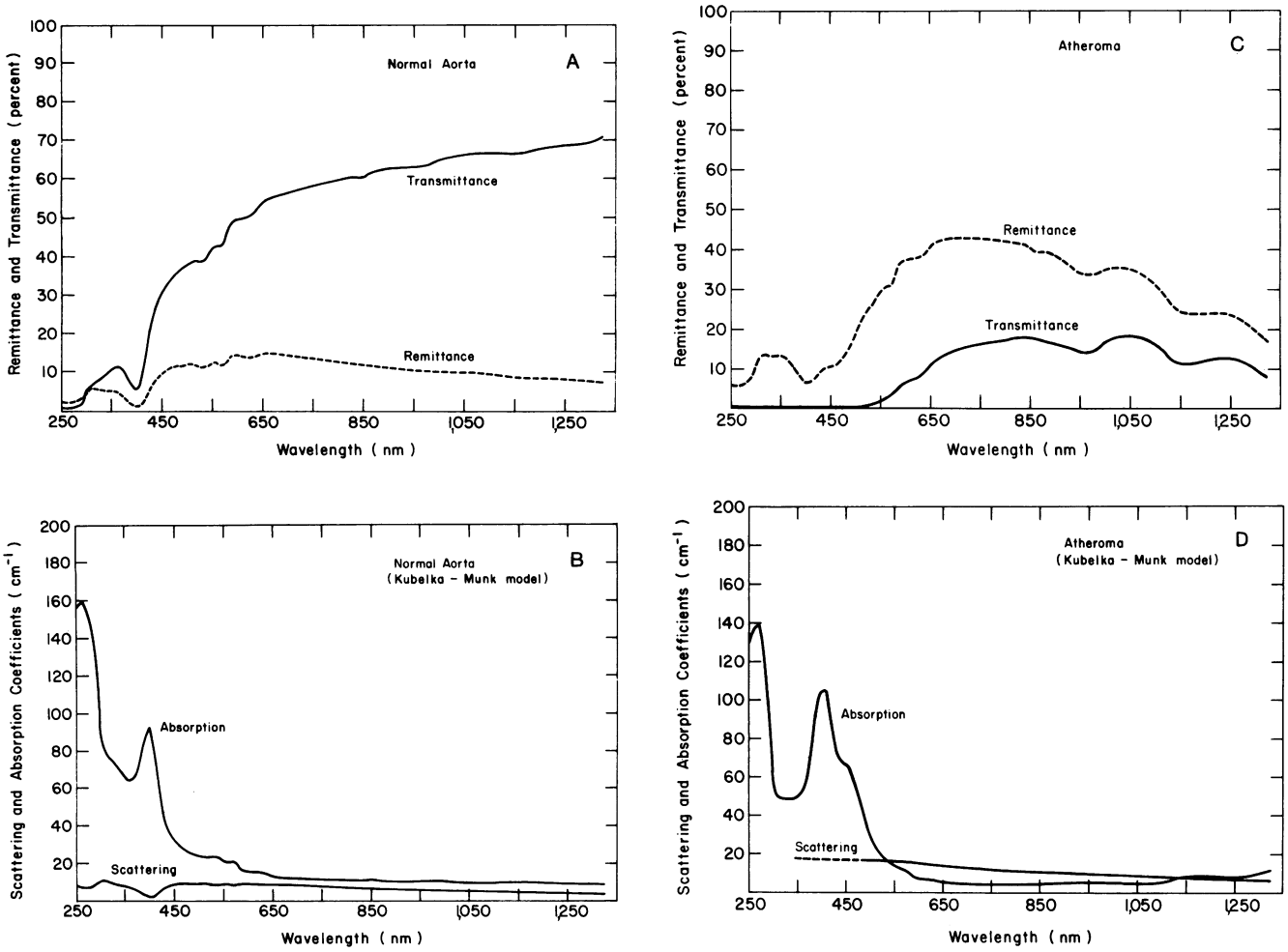

Figure 4. Optical properties of normal aorta. (*A*) Remittance and transmittance data for a typical specimen of normal cadaver aortic intima, 310 μm thick. (*B*) Calculated KM absorption and scattering coefficients for the same specimen. (*C*) Remittance and transmittance data for a typical atheroma, 1.5-mm thick (*D*) Calculated KM absorption and scattering coefficients. Note the absorption peaks corresponding to known tissue chromophores (hemoglobin at 550–570, 530–550, and 390–420 nm, aromatic amino acids, and DNA at 250–290 nm) and the extra absorbance for atheroma ~ 470 nm.

and atheroma measurements on a typical specimen. All of the atheromatous spots studied had greater absorption from 440–500 nm than all of the normal spots. The average Kubelka-Munk absorption coefficient for the twelve laser spectrophotometer measurements on atheromas from four individuals was 61±16 cm^{-1} while the average absorption of the uninvolved areas in the same specimens was 27±4 cm^{-1} (Table I). Beer's law analysis gave 48±9 cm^{-1} and 25±4 cm^{-1}, respectively (Table I).

Fig. 6 shows the ratio of atheroma to normal aorta absorption from 300–600 nm, for both integrating sphere and laser spectrophotometer measurements. This ratio is largest near 470 nm. For paired measurements (atheroma/normal) within the same specimen, the ratio of atheroma to normal tissue absorption at 470 nm ranged from 1.5–3.8 (Table I).

In the laser spectrophotometer data, differences in average absorbance between atheroma and normal tissue at 470 nm were statistically significant with $P < 0.05$ for both the KM and Beer's law analyses (Table I). In the integrating sphere data, comparing average absorbance of atheroma or normal from different individuals using an unpaired *t* test gave $P < 0.001$.

Scattering coefficients increased two- to threefold with decreasing wavelength over the spectral range studied, varying slowly and smoothly. In general, scattering was slightly higher in atheromas but always similar in spectral character to that of normal aorta. For thin specimens where *T* was large enough to use Eq. 3, as in Fig. 4 *B*, the scattering coefficient, *S*, was essentially constant at about 8 cm^{-1} from 425–550 nm. The flat behavior of *S* in this region justifies the approximation used for thick samples with small *T* (see Methods). In thicker specimens (Fig. 4 *C* and *D*) transmittance was <0.5% in some regions, requiring use of Eq. 5. In the waveband of preferential absorption, the scattering coefficient was smaller than the absorption coefficient, thus justifying the use of Beer's law (see Methods). The minima seen in Fig. 4 *B* at 260 and 400 nm are probably artifacts due to measurements at regions of high absorbance.

After thermal denaturation at 100°C there was a small increase in both absorption and scattering and reduced prominence of the Soret band, perhaps reflecting changes in collagen and hemoglobin (data not shown). These changes were small compared with the preferential absorption in atheromas.

During extraction with xylenes, the atheroma turned from

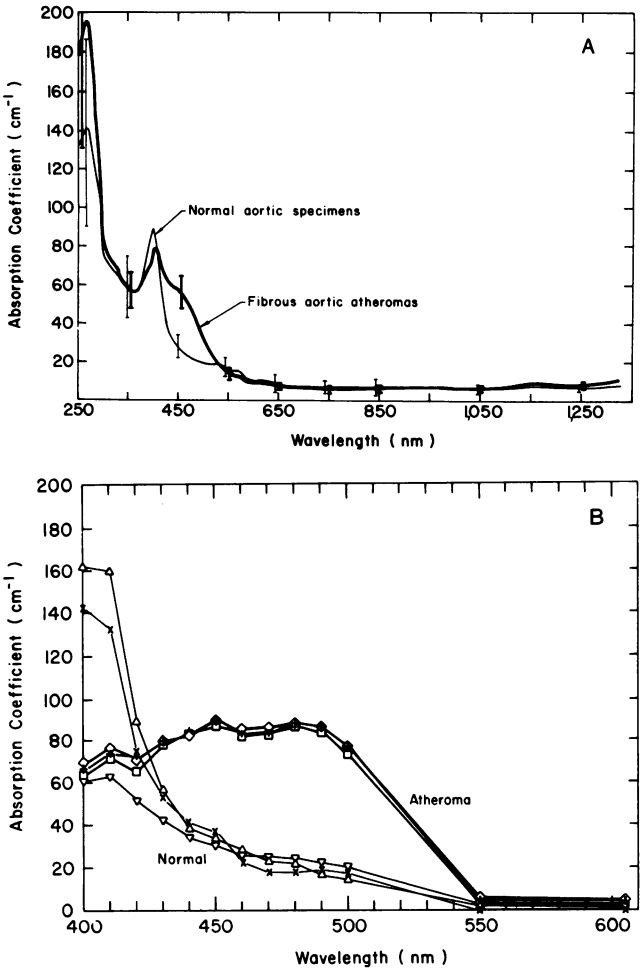

Figure 5. Comparison of absorption coefficients for atheromatous and normal aortic specimens. (*A*) The KM absorption coefficients were calculated from integrating sphere data and averaged for seven normal aortic specimens (thin line) and for six fibrous aortic atheromas (thick line). Bars indicate ±1 SD. (*B*) The KM absorption coefficients calculated with laser spectrophotometer data from three regions of atheroma (□, +, ◇, thick lines) and three adjacent normal regions (▽, ×, △, thin lines) from the same aorta. Note the spectral region from 420 to 530 nm where the atheroma absorption coefficient is greater than that of normal specimens.

yellow to white and the xylenes from clear to yellow. The absorbance of the atheroma extract before thin-layer chromatography is shown in Fig. 7, along with that of beta carotene, showing the two to be similar. The absorption at 400 nm and the large peak below 380 nm are probably due to other components and/or light scattering. Thin-layer chromatography of the atheroma extract yielded six bands with retardation factor (Rf) values of 0.25, 0.13, 0.12, 0.11, 0.01–0.10, and 0.0, respectively. Bands 1 and 2 had absorption peaks at 420, 440, and 470 nm (consistent with two isomers of beta carotene); band 4 had absorption peaks at 442, 470, and 500 nm (consistent with lycopene); and band 5 had absorption peaks at 440, 465, and 495 nm. The pigment in band 6 had peaks at 400, 422, 445, and 470 nm and may be a mixture of carotenoids. Band 3 had no significant absorption between 400–550 nm. Table II gives absorption peaks for carotenoids that are known to exist in humans.

Histologic analysis confirmed that the areas of specimens chosen to be normal had normal morphology. In the atheromas there was thickening of the intima with dense hyalinized collagen bundles and diminished amounts of elastic tissue and smooth muscle cells. In the centers of the atheromas there were variable amounts of irregularly deposited grumous material that appeared to consist of extracellular lipids and cellular debris. In some of the specimens there were scattered dystrophic calcifications. There was no evidence of ulceration or direct exposure of the grumous material to the luminal surface, although in two specimens there were scattered acute and chronic inflammatory cells in the superficial portion of the atheroma.

Discussion

Confinement of the effects of the laser radiation to the atheromatous material obstructing arteries has been a major challenge in laser angioplasty. This study employed two different measurement techniques to demonstrate a 450–500-nm waveband of significant preferential light absorption in fibro-fatty atheromas due to the presence of carotenoids. This suggests that selective laser ablation of atheromas could be accomplished by choosing a laser emitting in this waveband. It is possible to select laser parameters (pulse duration, spot size, intensity, and energy per pulse) which will ablate atheromas but have minimal effects on normal tissues (35).

The utility of the argon laser (emitting primarily at 514 and 488 nm) for ablating atheromas may reflect its partial overlap with this preferential absorption band. One could make the argon laser more selective by tuning to its 488-nm line or other lines in the region of preferential absorption. Even better results might be obtained from a flashlamp-pumped dye laser tuned to the wavelength of maximum selectivity with short pulses (<10 ms), which would minimize thermal diffusion damage to adjacent tissues (36).

Measuring absorption in biological materials is complicated by light scattering, which necessitates using a spectrophotometer that can collect the scattered light and using an optical model that takes scattering into account. One popular model is the KM formulation (see Methods) which ignores reflection and refraction at sample boundaries and assumes that inhomogeneities within the sample are small compared with thickness, that illumination is diffuse, and that scattering is symmetric. Although these assumptions are not entirely met by tissue, the KM model has been useful for studying skin (31–33), arteries (25), plants (37), and other biological materials. Some of these assumptions were addressed in this study by matching the index to the tissue to minimize surface effects and by using relatively thick specimens. Diffuse illumination was impractical, since it would have increased the spot size unacceptibly. The error from using collimated illumination is at most a factor of 2, and should be comparable for both atheroma and normal tissue (27). Although scattering may not have been isotropic, this possibility primarily affects the interpretation of the scattering coefficient. Any errors from inadequate modeling of scattering are likely to be small in the region of preferential absorption because absorption is much greater than scattering for both atheroma and normal aorta in that waveband. This is corroborated by the close agreement between the KM values for K and the Beer's law values for A_B, which ignore scattering. The results are similar to those of Kaminow (24), Anderson (31, 33), Wan (32), and van Gemert (25).

Table I. Absorption Data at 470 nm on Atheroma and Normal Aorta

Measurement data analysis	Atheroma	Normal	Significance	Ratio
	cm^{-1}	cm^{-1}	P	
Integrating sphere				
KM analysis	50±7* (6, 6)‡	24±4* (3, 7)‡	5.6×10^{-4}§	2.1‖
Beer's law analysis	63±7 (6, 6)	36±7 (3, 7)	5.7×10^{-3}	1.8
Laser spectrophotometer				
KM analysis	61±16 (4, 12)	27±14 (4, 12)	0.044	2.2 (1.5–3.8)¶
Beer's law analysis	48±9 (4, 12)	25±4 (4, 12)	0.039	1.9 (1.4–3.1)¶
Combined data				
KM analysis	54±12 (10, 18)	26±4 (7, 19)	2.4×10^{-5}	2.2
Beer's law analysis	57±11 (10, 18)	30±8(7, 19)	2.6×10^{-5}	1.9

* Mean±standard deviation. ‡ Parameters denote (No. of individuals, No. of different measurement sites). § P value is calculated by first calculating the average absorbance at all measurement sites for each tissue type in each individual and then treating each of those averages as a separate observation (see Methods). ‖ Mean atheroma absorbance/mean normal aorta absorbance. ¶ Range of ratios over the four individuals studied.

Our identification of the yellow atheroma chromophores as carotenoids supports the work of Blankenhorn (38–42), who demonstrated carotenoids within atheromas more than 20 yr ago and showed that the amount of carotenoid in atheromas increases with the severity of the lesion. They are ubiquitous in nature, giving the red and yellow coloring of many vegetables (tomatoes, carrots, squash), animal products (egg yolk, butter, chicken fat), and exotic animals (parrots, canaries) (43). Blankenhorn found that the carotenoid content in xanthomas can be increased about 30% by administration of low dose beta carotene (17 mg/d orally for 5 wk) (38). Patients with erythropoietic protoporphyria treated with oral doses of beta carotene (30–300 mg/d) often develop yellow coloration from cutaneous accumulation of carotenoids within a few weeks (44). Thus it may be possible to considerably increase the carotenoid content of atheromas using safe oral doses of these chromophores for short periods of time.

In laser angioplasty, the increased carotenoid concentrations could further accentuate the preferential absorption in atheromas, enhance the efficiency of atheroma ablation, and decrease the chance of damage to normal tissue. Since different carotenoids have different absorption peaks it may be possible to select the wavelength of maximum atheroma absorption in order to match it to laser emission lines (Table II).

Although only fibro-fatty atheromas were studied, preferential absorption would be expected in any yellow plaque. Some arterial obstructions, however, are not yellow and therefore may not contain significant levels of carotenoids. It is not yet known

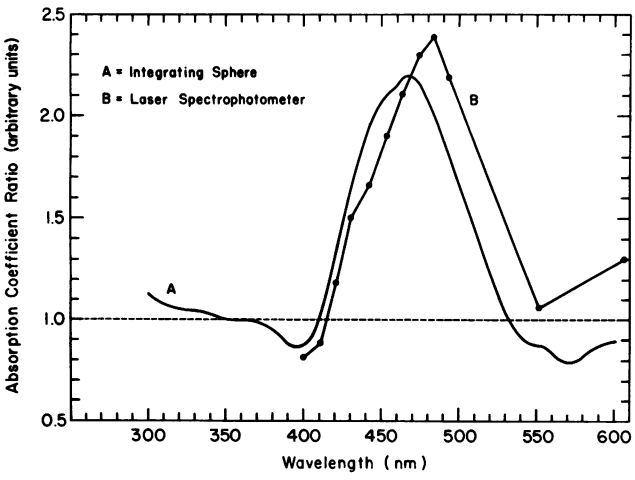

Figure 6. Waveband of preferential atheroma absorbance. The ratio of atheroma absorption to normal aorta absorption is plotted for both the integrating sphere and laser-based spectrophotometer data to demonstrate the region of selective light absorption in atheromas. Between 450 and 500 nm the average atheroma absorption is >1.7 times that of normal artery.

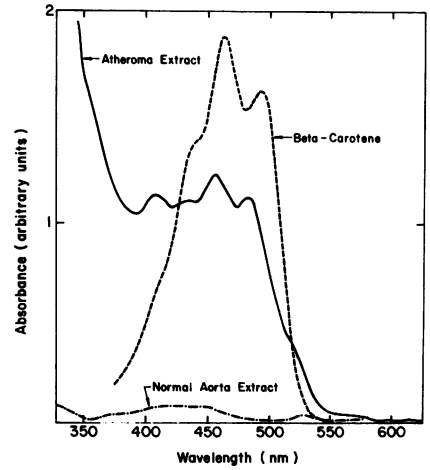

Figure 7. Absorption spectra of lipophilic chromophores extracted from atheroma and normal aorta. Chromophores extracted from atheromas absorb in the waveband where there is preferential absorption in atheromas. No chromophores extracted from normal aorta showed significant absorption in that waveband. Comparison of beta carotene absorption spectra with the atheroma extract spectra suggests that some of the extract could be beta carotene, a known constituent of atherosclerotic lesions.

Table II. Absorption of Carotenoids Known to Exist in Humans

Carotenoid	Absorption maxima in light petroleum
	nm
lycopene	446, 472, 505
beta carotene	425, 451, 480
canthaxanthin	466
alpha carotene	422, 444, 480
zeta carotene	378, 400, 425
lutein	420, 447, 477
cryptoxanthin	425, 451, 483
zeaxanthin	423, 451, 483
capsanthin	474–475, 504
capsorubin	444, 474, 506

if these lesions would accumulate exogenous carotenoids. There may also be differences in absorbance between normal aorta and normal small arteries, such as coronaries, due to differences in elastic tissue and smooth muscle content. Thrombotic lesions may still be successfully ablated because of the overlap of hemoglobin and carotenoid absorbance bands. It may be necessary to explore additional strategies to achieve a selective laser effect, including the use of tetracycline, which accumulates in atheromas and confers absorption near 350 nm (45); soluble dyes such as sudan black (3), or photosensitizers such as hematoporphyrin derivative (46). In general, however, it seems most reasonable to exploit existing absorbances when possible.

Acknowledgments

We thank the Arthur O. and Gullan M. Wellman Foundation for financial support, Laser Sciences Inc. for loan of the nitrogen-pumped dye laser, the Harvard School of Public Health Biostatistics Consulting Laboratory for assistance with the statistical analysis, and the Wellman Laboratory staff for their assistance with the research.

References

1. Marcuz, R., J. R. M. Martins, A. Tupinamba, E. A. Lopes, H. Vargas, A. F. Pena, V. B. Cravalho, and L. V. Decourt. 1980. Possibilidades terapeuticas do raio laser em ateromas. *Arq. Bras. Cardiol.* 34: 9–12.

2. Lee, G., R. Ikeda, J. Kozina, and D. T. Mason. 1981. Laser dissolution of coronary atherosclerotic obstruction. *Am. Heart J.* 102:1074–1075.

3. Abela, G. S., S. Normann, D. Cohen, R. L. Feldman, E. A. Geiser, and C. R. Conti. 1982. Effects of carbon dioxide, Nd:Yag and argon laser radiation on coronary atheromatous plaques. *Am. J. Cardiol.* 50: 1199–1205.

4. Choy, D. S. J., S. H. Stertzer, H. Z. Rotterdam, and M. S. Bruno. 1982. Laser coronary angioplasty: experience with 9 cadaver hearts. *Am. J. Cardiol.* 50:1209–1211.

5. Lee, G., R. Ikeda, I. Herman, R. M. Dwyer, M. Bass, H. Hussein, J. Kozina, and D. T. Mason. 1983. The qualitative effects of laser irradiation on human arteriosclerotic disease. *Am. Heart J.* 105:885–889.

6. Geshwind, H., G. Boussignac, B. Teisseire, D. Laurent, N. Benaiem, A. Gaston, and J. P. Becquemin. 1983. Laser angioplasty: effects on coronary artery stenosis. *Lancet.* ii:1134.

7. Linsker, R., R. Srivansan, J. J. Wynne, and D. R. Alonso. 1984. Far-ultraviolet laser ablation of atherosclerotic lesions. *Lasers Surg. Med.* 4:201–206.

8. Lee, G., R. M. Ikeda, D. Stobbe, C. Ogata, M. C. Chan, D. L. Seckinger, A. Vazquez, J. Theis, R. L. Reis, and D. T. Mason. 1983. Effects of laser irradiation on human thrombus: demonstration of a linear dissolution-dose relation between clot length and energy density. *Am. J. Cardiol.* 52:876–877.

9. Lee, G., R. M. Ikeda, M. C. Chan, J. Dukich, M. H. Lee, J. H. Theis, W. J. Bommer, R. L. Reis, E. Hanna, and D. T. Mason. 1984. Dissolution of human atherosclerotic disease by fiberoptic laser-heated metal cautery cap. *Am. Heart J.* 107:777–778.

10. Gerrity, R. G., F. D. Loop, L. A. R. Golding, L. A. Ehrhart, and Z. B. Argenyi. 1983. Arterial response to laser operation for removal of atherosclerotic plaques. *J. Thorac. Cardiovasc. Surg.* 85:409–421.

11. Lee, G., R. M. Ikeda, J. H. Theis, M. C. Chan, D. Stobbe, C. Ogata, A. Kumagai, and D. T. Mason. 1984. Acute and chronic complications of laser angioplasty: vascular wall damage and formation of aneurysms in the atherosclerotic rabbit. *Am. J. Cardiol.* 53:290–293.

12. Lee, G., R. M. Ikeda, R. M. Dwyer, H. Hussein, P. Dietrich, and D. T. Mason. 1982. Feasibility of intravascular laser irradiation for in vivo visualization and therapy of cardiocirculatory diseases. *Am. Heart J.* 103:1076–1077.

13. Lee, G., D. Seckinger, M. C. Chan, A. Embi, D. Stobbe, R. V. Thomson, N. A. Sanchez, R. M. Ikeda, R. L. Reis, and D. T. Mason. 1984. Potential complications of coronary laser angioplasty. *Am. Heart J.* 108:1577–1579.

14. Ward, H. 1984. Laser recannalization of atheromatous vessels using fiber optics. *Lasers Surg. Med.* 4:353–363.

15. Abela, G. S., S. J. Normann, D. M. Cohen, D. Franzini, R. L. Feldman, F. Crea, A. French, C. J. Pepine, and R. C. Conti. 1985. Laser recanalization of occluded atherosclerotic arteries in vivo and in vitro. *Circulation.* 71:403–411.

16. Lee, G., R. M. Ikeda, M. C. Chan, D. Stobbe, J. Kozina, M. C. Jiang, R. L. Reis, and D. T. Mason. 1985. Current and potential uses of lasers in the treatment of atherosclerotic disease. *Chest.* 3:429–434.

17. Choy, D. S., S. Stertzer, H. Z. Rotterdam, N. Sharrock, and I. P. Kaminow. 1982. Transluminal laser catheter angioplasty. *Am. J. Cardiol.* 50:1206–1208.

18. Eldar, M., A. Battler, H. N. Neufeld, E. Gaton, R. Arieli, S. Akselrod, A. Levite, and A. Katzir. 1984. Transluminal carbon dioxide laser catheter angioplasty for dissolution of atherosclerotic plaques. *J. Am. Coll. Cardiol.* 3:135–137.

19. Ginsberg, R., D. S. Kim, D. Guthaner, J. Toth, and R. S. Mitchell. 1984. Salvage of an ischemic limb by laser angioplasty: description of a new technique. *Clin. Cardiol.* 7:54–58.

20. Choy, D. S. J., S. H. Stertzer, R. D. Myler, J. Marco, and G. Fournay. 1984. Human coronary laser recanalization. *Clin. Cardiol.* 7: 377–381.

21. Geshwind, H., G. Boussignac, B. Teisseire, C. Vielledent, A. Gatson, J. P. Becquemin, and P. Mayiolini. 1984. Percutaneous transluminal laser angioplasty in man. *Lancet.* i:844.

22. Geshwind, H. J., G. Boussignac, B. Teisseire, N. Benhaiem, R. Bittoun, and D. Laurent. 1984. Conditions for effective Nd-YAG laser angioplasty. *Br. Heart J.* 52:484–489.

23. Ginsberg, R., L. Wexler, R. S. Mitchell, and D. Profitt. 1985. Percutaneous transluminal laser angioplasty for treatment of peripheral vascular disease clinical experience with 16 patients. *Radiology.* 156: 619–24.

24. Kaminow, I. P., J. M. Weisenfeld, and D. S. J. Choy. 1984. Argon laser disintegration of thrombus and atherosclerotic plaque. *Appl. Optics.* 23:1301–1302.

25. van Gemert, M. J. C., G. A. C. M. Schets, E. G. Stassen, G. H. M. Gijsbers, and J. J. Bonnier. 1985. Optical properties of human blood vessel wall and plaque. *Lasers Surg. Med.* 5:235–238.

26. Kubelka, P., and F. Munk. 1931. Ein Beitrag zur Optik der Farbanstriche. *Z. Technichse.* 12:593–601.

27. Kubelka, P. 1948. New contributions to the optics of intensely light-scattering materials. Part I. *J. Opt. Soc. Am.* 38:448–457.

28. Kubelka, P. 1954. New contributions to the optics of intensely light-scattering materials. Part II: nonhomogeneous layers. *J. Opt. Soc. Am.* 44:330–335.

29. Kortum, G. 1969. Reflectance Spectroscopy. Springer-Verlag, Inc., New York. 15–87.

30. Prince, M. R., J. A. Parrish, T. F. Deutsch, A. R. Oseroff. 1985. Tissue spectroscopy with a pulsed tunable dye laser. *Proc. Assoc. Adv. Med. Instrumen.* 20:72.

31. Anderson, R. R., J. Hu, and J. A. Parrish. 1981. Optical radiation transfer in the human skin and application in in vivo remittance spectroscopy. *Proc. Symp. Bioengineering Skin.* 245–257.

32. Wan, S., R. R. Anderson, and J. A. Parrish. 1981. Analytical modeling for the optical properties of the skin with in vitro and in vivo applications. *Photochem. Photobiol.* 34:493–499.

33. Anderson, R. R., and J. A. Parrish. 1981. The optics of human skin. *J. Invest. Derm* 77:13–19.

34. Welch, A. J. 1985. The thermal response of laser irradiated tissue. *IEEE (Inst. Electr. Electron. Eng.) J. Quantum Electronics.* QE20:1471–1481.

35. Prince, M. R. 1985. Selective laser ablation of atheromatous arterial obstructions (M.D. thesis). Harvard Medical School, Countway Library, Cambridge, MA. 19–22.

36. Anderson, R. R., and J. A. Parrish. 1983. Selective photothermolysis: precise microsurgery by selective absorption of pulsed radiation. *Science (Wash. DC).* 220:524–527.

37. Kazarinova-Fukshansky, N., M. Seyfried, and E. Schafer. 1985. Distortion of action spectra in photomorphogenesis by light gradients within the plant tissue.

38. Blankenhorn, D. H. 1960. The infiltration of carotenoids into human atheromas and xanthomas. *Ann. Intern. Med.* 53:944–954.

39. Blankenhorn, D. H., D. G. Freiman, and H. C. Knowles. 1958. Carotenoids in man. The distribution of epiphasic carotenoids in atherosclerotic lesions. *J. Clin. Invest.* 35:1243–1247.

40. Blankenhorn, D. H., and H. Braunstein. 1958. Carotenoids in man. III. The microscopic pattern of fluorescence in atheromas and its relation to their growth. *J. Clin. Invest.* 37:160–165.

41. Blankenhorn, D. H. 1957. Cartenoids in man IV. Carotenoid stores in normal adults. *J. Biol. Chem.* 229:809–816.

42. Blankenhorn, D. H. 1957. Carotenoids in man II. Fractions obtained from atherosclerotic and normal aortas, serum, and depot fat by separation on alumina. *J. Biol. Chem.* 227:963–973.

43. Bauernfeind, J. C. 1981. Carotenoids as Colorants and Vitamin A Precursors. Academic Press, Inc., New York. 938.

44. Mathews-Roth, MM. 1981. Carotenoids in medical applications. *In* Carotenoids as Colorants and Vitamin A Precursors. J. C. Bauernfeind, editor. Academic Press, New York. 755–785.

45. Murphy-Chutorian, D., J. Kosek, W. Mok, S. Quay, W. Huestes, J. Mehigan, D. Profitt, and R. Ginsberg. 1985. Selective absorption of ultraviolet laser energy by human atherosclerotic plaque treated with tetracycline. *Am. J. Cardiol.* 55:1293–1297.

46. Spears, J. R., J. Serur, D. Shropshire, and A. Paulin. 1983. Fluorescence of experimental atheromatous plaques with hematoporphyrin derivative. *J. Clin. Invest.* 71:395–399.